# Evaluation of Hybrid Polarimetric Decomposition Techniques for Forest Biomass Estimation

Kiledar S. Tomar, Shashi Kumar, and Valentyn A. Tolpekin

***Abstract*—Forest plays an important role in carbon sequestration and biosphere-atmosphere interaction. Knowledge of forest biomass content helps in assessing its sustainability and thus mitigating climate change. The advancement in remote sensing technology provides the capability of estimating biomass at a large scale. Hybrid polarimetry has gained significant attention among other radar missions due to its fundamental advantages. In this article, the potential of hybrid polarimetric SAR is evaluated for the efficient forest aboveground biomass (AGB) estimation for Barkot Forest, Uttarakhand, India. Forest biomass is calculated by means of the extended water cloud model. Scattering parameters are derived using two widely used hybrid polarimetric decomposition techniques, m$-\delta$ and m–$\chi$ decompositions. Potential insight into the efficacy of these decomposition techniques toward biomass estimation is brought forth. The modeled AGB estimates were compared with fully polarimetric data-based estimated AGB. The estimation based on the m–$\chi$ and m$-\delta$ decomposition resulted in biomass estimation with an accuracy of 75.8% and 73.4%, respectively.**

***Index Terms*—Aboveground biomass (AGB), hybrid polarimetric (Hybrid Pol) SAR, RISAT-1.**

## I. Introduction

ABOVEGROUND biomass (AGB) content in the forest is essential for understanding and modeling ecosystem dynamics and thus mitigating climate change. Field-based approaches are often used to estimate forest biomass [1], [2]. However, they are limited to small spatial and temporal coverage. Remote sensing has been widely used for forest monitoring activities. Due to its high spatial and temporal coverage, remote sensing-based methods can provide spatial information on AGB at large scales. Various remote sensing technology has been exploited to retrieve the forest AGB.

Manuscript received January 31, 2019; revised June 30, 2019 and September 30, 2019; accepted October 9, 2019. Date of publication October 31, 2019; date of current version November 22, 2019. (*Corresponding author: Shashi Kumar.*)

K. S. Tomar was with the Indian Institute of Remote Sensing, Indian Space Research Organisation, Dehradun 248001, India, and ITC, 997414, Hengelosestraat, The Netherlands. He is now with the Laboratory of Polar Remote Sensing, National Centre for Polar and Ocean Research, Vasco-da-Gama 403804, India (e-mail: kdsingh108@hotmail.com).

S. Kumar is with the Department of Photogrammetry and Remote Sensing, Indian Institute of Remote Sensing, Indian Space Research Organisation, Dehradun 248001, India (e-mail: shashi@iirs.gov.in).

V. A. Tolpekin is with the Faculty of Geo-Information Science and Earth Observation (ITC), University of Twente, 997414 Hengelosestraat, The Netherlands (e-mail: tolpekin@itc.nl).

Color versions of one or more of the figures in this article are available online at http://ieeexplore.ieee.org.

Digital Object Identifier 10.1109/JSTARS.2019.2947088

Optical remote sensing has certain limitations in detecting the forest structure under cloud or haze due to the use of short wavelengths that cannot penetrate through cloud and haze. It is also known to give saturated signatures with increasing biomass for dense canopies. Furthermore, it only identifies the canopy surface and not the underlying volume. Radar as an active sensor transmits its own signal in the form of an electromagnetic wave that makes it independent of solar illumination and also the longer wavelengths enable a deeper penetration through the dense forest canopy. This interaction of microwaves with forest canopy can be characterized as an interaction with the semitransparent medium. SAR polarimetry deals with information retrieval from different scatterers using the different polarizations of electromagnetic waves. This information from backscatter can be decomposed into different components to interpret distributed target [3].

Polarimetric SAR systems have the capacity of separating the contributions of different scattering elements available in a single SAR resolution cell. The scattering elements commonly used in forest studies are surface scattering, volume scattering, and double-bounce scattering. The incoherent decomposition model was introduced by Freeman and Durden [4] for the decomposition of these scattering mechanisms from the targets. Studies have implemented these decomposition methods for a variety of applications [5], [6]. It was further developed and modified by Yamaguchi was known as Yamaguchi four-component decomposition that includes helix scattering mostly suitable for complex urban structures [7]. Due to terrain slope variation, a shift occurs in the polarization orientation angle (POA) of the fully polarized SAR data. In addition to this, the random orientation of forest structure causes a shift in orientation angle of polarization ellipse. This POA shift affects the polarimetric radar signatures and shows an overestimation of volume scattering and underestimation of double-bounce scattering after the decomposition of forest parameters, such as stem volume and biomass, and can be recovered by deorientation [8]–[11].

Hybrid Polarimetric (Hybrid Pol) mode provides some fundamental advantages over fully polarimetric SAR and has been implemented for different applications [12]–[14]. These radar systems come with a lower hardware cost and are relatively easy to implement. Transmission of the wave in a circularly polarized manner which produces backscattering that is rotationally invariant and eliminating the POA shift removal process. Hybrid Pol systems transmit circularly polarized waves and receive two orthogonal mutually coherent polarizations. In addition to

TABLE I
HYBRID AND FULLY POLARIMETRIC DATASET ACQUIRED OVER BARKOT FOREST

| **Satellite** | RISAT-1 | RADARSAT-2 |
|---|---|---|
| **Date of acquisition** | Jul. 1st, 2013 | Jan. 28th, 2014 |
| **Operated frequency** | *C*-band | *C*-band |
| **Wavelength** | 5.6 cm | 5.5 cm |
| **Data format** | SLC | SLC |
| **Mode** | FRS-1 | Fine quadpol |
| **Polarization** | Hybrid pol | Quadpol |
| **Resolution** | 2.34 m × 3.33 m | 5.2 m × 7.7 m |

that, it is unaffected by the POA shift. This provides us with a ripe opportunity to use Hybrid PolSAR data to identify the contribution to total backscatter from different scatterers for the estimation of AGB.

In this article, hybrid polarimetry based scattering retrieval (from m$-\delta$ and m$-\chi$ decomposition) has been utilized for extended water cloud model (EWCM). The hybrid polarimetry-based AGB estimates is compared with a fully polarimetric model-based AGB estimates. The aim is to provide a novel framework utilizing the scattering mechanism retrieved from m$-\delta$ and m$-\chi$ Hybrid Pol modeling in the EWCM to estimate the forest AGB. In addition to the water cloud model (WCM), scattering from the ground-stem interaction has been considered with the help of the capability of polarimetric SAR. Earlier studies based on the WCM have been reported to retrieve the model parameters with the help of field datasets for calibration. The proposed framework is believed to have less dependence on the field datasets for the model calibration.

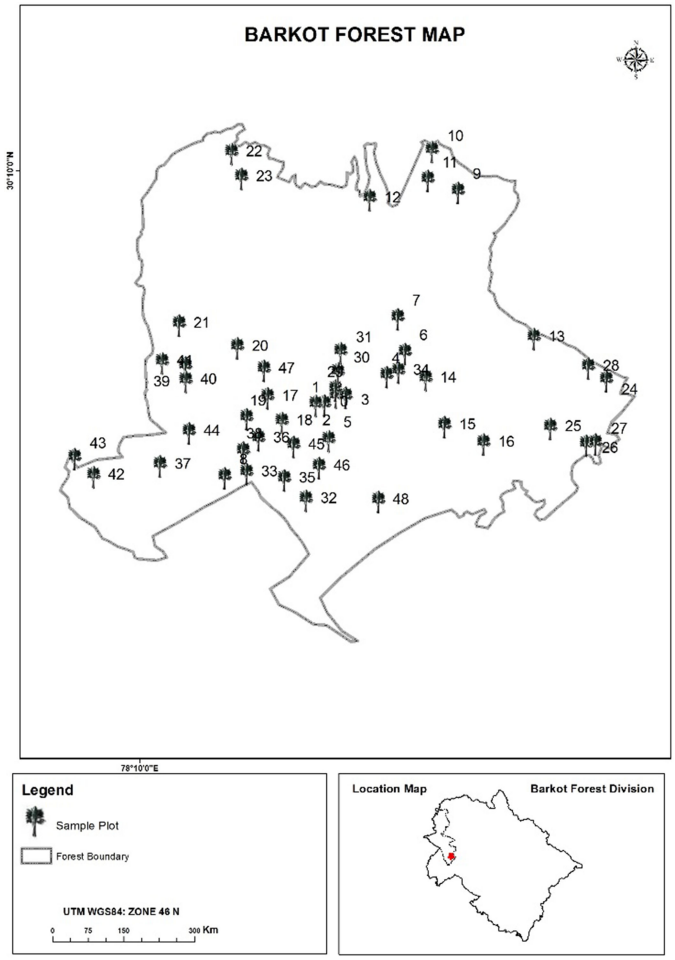


Fig. 1. Study area and distribution of sample plots (with Plot ID) in the Barkot Forest area.

## II. STUDY SITE AND DATASET

To study the potential of Hybrid PolSAR for AGB, Barkot Forest (Uttarakhand, India) is chosen as the study site. It is located between Gharwal and Shivalik ranges of the Himalayas. The geographical coordinates lie in between 29°33'–30°00' N latitude and 78°18'–79°49' E longitude. This forest is moderately dense and Sal (*Shorea robusta*) dominated moist deciduous forest. Sal trees which are dominant species assisted with Teak (*Tectona grandis*), Sisoo (*Dalbergia sisoo*), and Khair (*Senegalia catechu*). Some other trees which also have a contribution to this forest are Rohini (*Mallotus philippensis (Lamk) Muell.-Arg.*), Chamror (*Ehretia laevis Roxb.*), Kanju (*Holoptelea integriflora (Roxb.) Planch.)* and Sagaun (*Tectona grandis L.f.*). Sal trees have about 40% contribution as dominating species to this forest area. This forest range is part of the Doon valley forest. The topography here is flat with very less undulations and does not lie in the hilly terrain. In this article, the right circular transmit mode data from RISAT-1 sensor and fully polarimetric data of RADARSAT-2 were utilized. These SAR sensor data were present in single look complex (SLC) format. Specifications pertaining to the dataset are given in Table I.

There was a total of 49 sample plots available in the Barkot Forest range. These plots were present in Sal and mixed Sal forest. The average tree height of these plots is approximately 25 m ranging from 23 to 30 m and DBH ranges from 24 to 62 cm. Available sample plots represent a standard square shape of 0.1 ha. The distribution of a sample plot is shown in Fig. 1.

## III. HYBRID POL DECOMPOSITION MODELING

The parameters required for EWCM to estimate the AGB were obtained through Hybrid Pol decomposition models. These parameters are the scattering information which can be expressed through stokes parameters and their child products.

### A. Stokes Parameter

Representation of Stokes parameters ($S_1$, $S_2$, $S_3$, $S_4$) has primarily two advantages that the parameters are measured in terms of their intensities and have the capability of delivering partially polarized waves in the form of $2 \times 2$ complex Hermitian positive semidefinite wave coherency matrix [$J$] and can be

expressed as follows:

$$[J] = \begin{bmatrix} \langle E_H E_H^* \rangle & \langle E_H E_V^* \rangle \\ \langle E_V E_H^* \rangle & \langle E_V E_V^* \rangle \end{bmatrix} = \frac{1}{2} \begin{bmatrix} S_1 + S_2 & S_3 + jS_4 \\ S_3 - jS_4 & S_1 - S_2 \end{bmatrix}. \tag{1}$$

The Stokes parameters in circular and linear polarization at the receiver can also be expressed as follows:

$$S_1 = \left\langle |E_{RH}|^2 + |E_{RV}|^2 \right\rangle \tag{2}$$

$$S_2 = \left\langle |E_{RH}|^2 - |E_{RV}|^2 \right\rangle \tag{3}$$

$$S_3 = 2\mathrm{Re} \left\langle E_{RH} E_{RV}^* \right\rangle \tag{4}$$

$$S_4 = -2\mathrm{Im} \left\langle E_{RH} E_{RV}^* \right\rangle \tag{5}$$

where $\mathrm{Re}$ and $\mathrm{Im}$ refers to the real and imaginary value of the horizontal and vertical receive polarization. Decomposition-specific parameters such as degree of polarization (DoP) (m), relative phase (d), and ellipticity parameter (x) further retrieved using Stokes parameters as follows:

$$m = \frac{\sqrt{s_2^2 + s_3^2 + s_4^2}}{s_1} \tag{6}$$

$$\delta = \tan^{-1}\left(\frac{s_4}{s_3}\right) \tag{7}$$

$$\sin(2\chi) = -\frac{s_4}{m s_1}. \tag{8}$$

### B. M-Chi Decomposition

The *m*-$\chi$ decomposition is obtained by utilizing a DoP, an ellipticity parameter, and the Stokes first parameter ($S_1$). The DoP indicates diffused scattering while $\chi$ is an indicator of even versus odd scattering as the sign of $\chi$ is an unambiguous indicator of even-versus-odd-bounce scattering. The ($\chi$) enters in this decomposition modeling in the form of the degree of circularity. The *m*-chi decomposed scattering element can be expressed as follows:

$$f_{\mathrm{odd}(m-\chi)} = \sqrt{s_1 \cdot m \cdot \frac{1 + \sin(2\chi)}{2}} \tag{9}$$

$$f_{\mathrm{even}(m-\chi)} = \sqrt{s_1 \cdot m \cdot \frac{1 - \sin(2\chi)}{2}} \tag{10}$$

$$f_{\mathrm{volume}(m-\chi)} = \sqrt{s_1 \cdot (1 - m)} \tag{11}$$

where $f_{\mathrm{odd}(m-\chi)}$, $f_{\mathrm{even}(m-\chi)}$, and $f_{\mathrm{volume}(m-\chi)}$ indicate the relative contribution of surface scattering, double-bounce scattering, and volume scattering, respectively, retrieved from *m*–$\chi$ decomposition.

### C. M-Delta Decomposition

The practical applicability of (*m*-$\delta$) decomposition is earlier introduced by Raney [10]. The *m*-delta decomposition comprises of the DoP (m), Stokes first parameter ($S_1$), and relative phase ($\delta$) derived from the Stokes parameter. The DoP indicates the polarized and diffused scatterings. The relative phase (here phase between *RH* and *RV*) represents the double-bounce scattering. Thus, the combination of DoP and relative phase is capable of characterizing the polarization state of the electromagnetic wave.

The scattering element retrieved from *m*-$\delta$ decomposition can be expressed as follows:

$$f_{\mathrm{odd}(m-\delta)} = \sqrt{s_1 \cdot m \cdot \frac{1 + \sin(\delta)}{2}} \tag{12}$$

$$f_{\mathrm{even}(m-\delta)} = \sqrt{s_1 \cdot m \cdot \frac{1 - \sin(\delta)}{2}} \tag{13}$$

$$f_{\mathrm{volume}(m-\delta)} = \sqrt{s_1 \cdot (1 - m)} \tag{14}$$

where the relative contribution of surface, double-bounce, and volume scatterings is indicated as $f_{\mathrm{odd}(m-\delta)}$, $f_{\mathrm{even}(m-\delta)}$, and $f_{\mathrm{volume}(m-\delta)}$, respectively.

## IV. Modeling the AGB

The concept of relating forest biophysical parameters and the retrieved backscatter from vegetation to model the AGB is given by WCM. The basic premise of WCM is that the vegetation acts as a homogenous medium occupied by the droplets of water and consider these droplets to be uniformly dispersed over a horizontal plane surface that signifies the ground surface. WCM does not consider the higher order scattering like even-bounce scattering, which also occurs from the forest. This WCM, further extended includes canopy gaps for higher order interactions for the vegetation cover (EWCM), has been used in this article.

### A. Extended Water Cloud Model

In the WCM, the surface and volume scatterings are involved whereas the ground-stem interaction was not included here. However, the ground-stem interaction also has some influence in the modeling of AGB as it is a part of the scattering mechanism held in the forest area. The EWCM includes the ground–stem interaction (double-bounce scattering), which is not available in the conventional WCM. There are a total of five unknown parameters in the EWCM**.** These are backscattering from canopy cover ($\sigma^0_{\mathrm{veg}}$), backscattering from the ground-to-stem interactions or stem-to-ground interactions ($\sigma^0_{gs}$), backscattering from the ground surface ($\sigma^0_{gr}$), total backscattering from forest ($\sigma^0_{\mathrm{for}}$), empirically defined coefficient ($\beta$), and AGB ($B_{\mathrm{AGB}}$). Polarimetric decomposition algorithms are used to calculate parameters, such as $\sigma^0_{\mathrm{veg}}$, $\sigma^0_{gs}$, $\sigma^0_{gr}$, and $\sigma^0_{\mathrm{for}}$, which reduces the number of unknown parameters to one, i.e., ($\beta$). This empirically defined the coefficient that helps in calculating the required AGB. In this article, the required backscattering parameters of EWCM have been retrieved using the *m*-delta and *m*-chi decompositions. The retrieved backscattering is from their respective volume, double bounce, and surface targets. Similarly, the empirically defined coefficient ($\beta$) has been derived from *in situ* measurements in the Barkot Forest area. From a number of field measurements, a total of 49 plots were available to perform this article out of which 15 sample plots have been taken into account to calculate the parameter $\beta$. Remaining sample plots were retained to perform the estimation of AGB.

Those plots that were used to calculate the $\beta$ parameter are mostly those plots that show less volume scattering with high biomass. To calculate $\beta$, the same plots are used for both the decomposition techniques. The relation of $\beta$ parameter with the scattering components, field measured AGB (*in situ* measurements), and the total backscatter from the forest can be given by simplifying (13) as

$$\beta = -\frac{1}{B_{\mathrm{AGB}}} \ln\left(\frac{\sigma^0_{\mathrm{for}} - \sigma^0_{\mathrm{veg}}}{\sigma^0_{gr} - \sigma^0_{\mathrm{veg}} + \sigma^0_{gs}}\right) \tag{15}$$

where $B_{\mathrm{AGB}}$ represents the AGB (t·ha$^{-1}$). In this article, for the estimation of $\beta$, it was assumed that the double-bounce scattering occurs from the vegetation (in the case of a forest). As the *C*-band data were used to perform the study which has a low canopy penetration ability than *L*-band. Hence, the backscatter from the ground–stem interactions is added to the backscatter from the vegetation that turned (16) as

$$\beta = -\frac{1}{B_{\mathrm{AGB}}} \ln\left(\frac{\sigma^0_{\mathrm{for}} - \left(\sigma^0_{\mathrm{veg}} + \sigma^0_{gs}\right)}{\sigma^0_{gr} - \sigma^0_{\mathrm{veg}} + \sigma^0_{gs}}\right). \tag{16}$$

The unit of $\beta$ parameter is ha/m$^3$ and it is represented in the terms of backscattering [15], [16] as

$$\sigma^0_{\mathrm{for}} = \sigma^0_{gr} e^{-\beta B_{\mathrm{AGB}}} + \sigma^0_{\mathrm{veg}}\left(1 - e^{-\beta B_{\mathrm{AGB}}}\right) + \sigma^0_{gs} e^{-\beta B_{\mathrm{AGB}}} \tag{17}$$

where $\sigma^0_{\mathrm{for}}$ represents the total backscatter from the forest, $\sigma^0_{gr}$ represents the backscatter from the ground, $\sigma^0_{\mathrm{veg}}$ represents the backscatter from canopy cover, $\sigma^0_{gs}$ represents the backscatter obtained from the ground–stem interaction, $B_{\mathrm{AGB}}$represents the AGB, and $\beta$ is the empirically defined coefficient. Helix scattering is almost negligible in forest areas as it is observed in complex urban structures. The empirically defined coefficient has been calculated from the field measured biomass and this coefficient and different backscatter were utilized to model the AGB. The overall methodology is shown in Fig. 2.

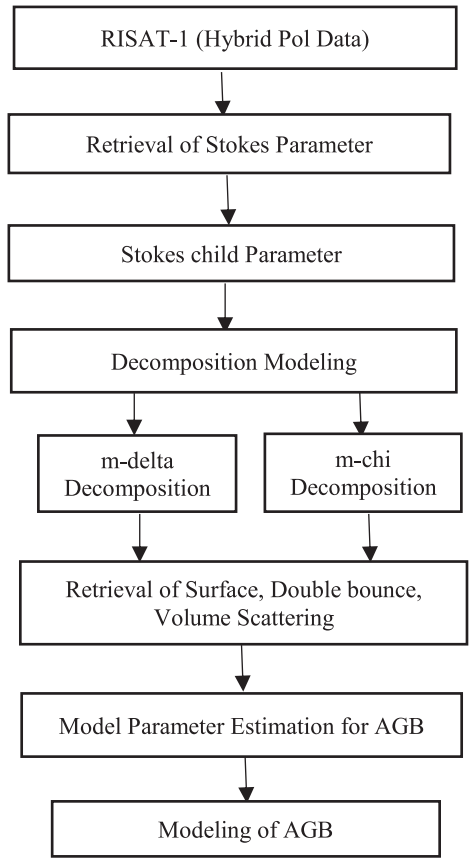


Fig. 2. Methodology followed to estimate forest biomass using RISAT-1 dataset.

## V. Results and Discussion

Out of 49 plots available from *in situ* measurements, 15 plots were taken to estimate the semiempirically defined coefficient. Remaining 34 plots were used to estimate the AGB. The estimated $\beta$ values of 15 plots from the *m*-delta and *m*-chi decompositions are 0.003019 and 0.003542, respectively. The estimated $\beta$ value for all the remaining sample plots (34 plots) is kept constant as per their polarimetric decomposition. Two decomposition models were used for the Hybrid Pol RISAT-1 data, namely, *m*-d, *m*–$\chi$, and were compared with the fully polarimetric decomposition (Yamaguchi decomposition) model. For each of the decomposition technique, scattering elements were obtained (see Fig. 3). For the given study area, the volume scattering dominates the surface scattering and the double-bounce scattering for the *m*-d, *m*–$\chi$, and Yamaguchi decomposition techniques at each sample plot, as shown in Fig. 3(a)–(c).

Also, the double-bounce scattering was observed to be minimum for all decomposition techniques. This is due to the fact that the present study area is dominated by the dense forest. Hence, most of the scattering occurs in the upper canopy layer.

The *m*-delta, *m*-chi, and Yamaguchi decomposed images of different scatterings obtained from the Barkot Forest area are shown in Fig. 4(a)–(c).

The backscatter value of volume scattering for both Hybrid Pol decomposition models is the same. The reason is that DoP (m) is a sensitive indicator of volume scattering, which is same for both decompositions. The Barkot Forest area is densely packed with the canopy cover. Hence, the incoming *C*-band waves first interact with the top canopy layer giving high values for the volume scattering. On the other hand, some of the waves may penetrate through the canopy layer and the double-bounce scattering occurs due to the ground-stem interactions or the stem-ground interactions. For higher wavelengths (like *L*-band and *P*-band), more double-bounce and surface scatterings could be expected for the same region. However, the present article restricted to the *C*-band dataset to estimate the AGB. Due to the canopy gaps, surface scattering may also occur. But the present study area is composed of dense forest; hence, volume scattering is dominating.

The parameters required for AGB calculation were determined from the polarimetric decomposition techniques. The AGB was calculated with the help of the semiempirical model (EWCM) and was compared with the field data (see Fig. 5).

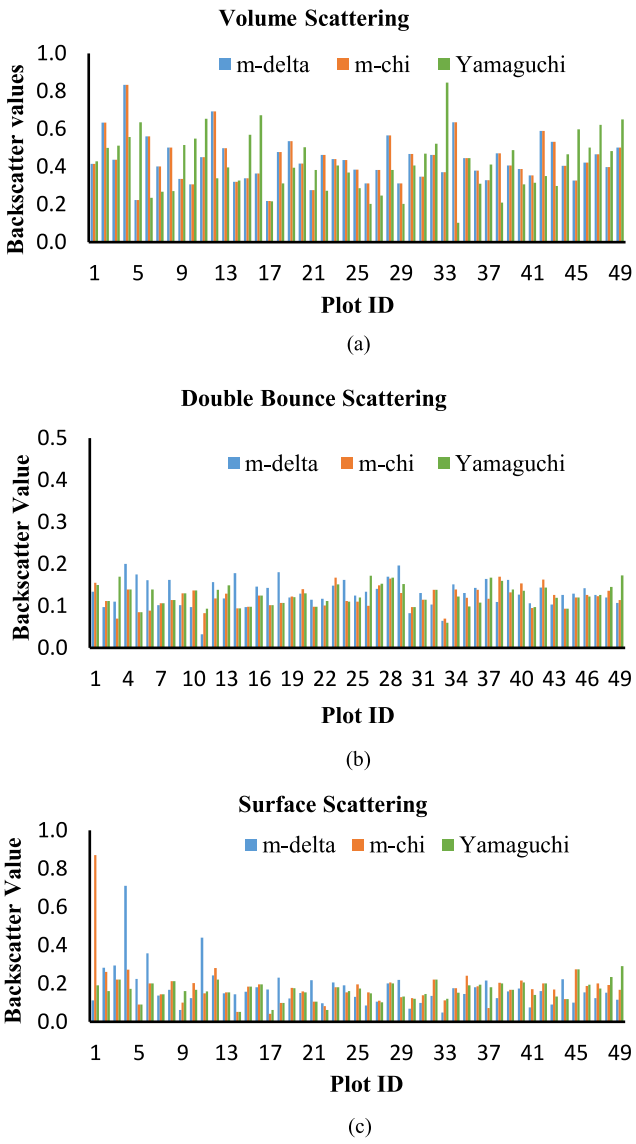


Fig. 3. Comparison of (a) volume, (b) double-bounce, and (c) surface scatterings obtained from *m*-delta, *m*-chi, and Yamaguchi decomposition models.

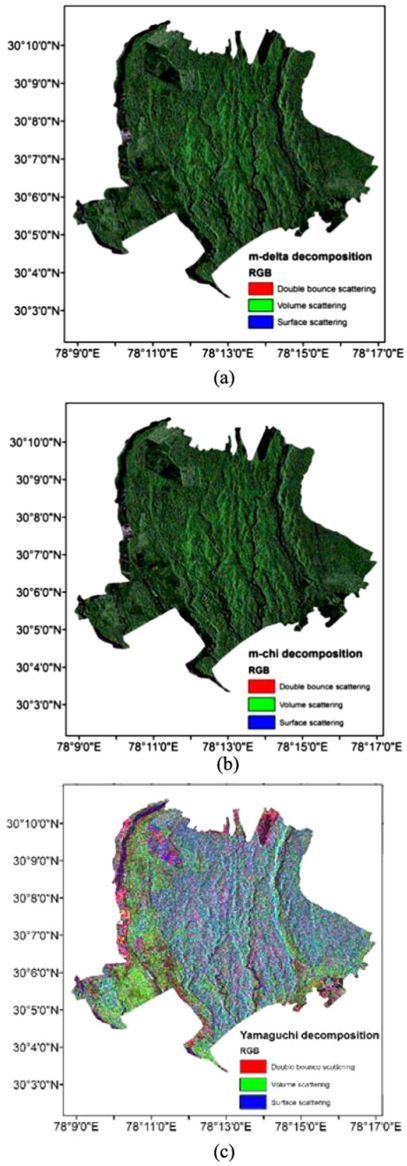


Fig. 4. (a) *m*-delta, (b) *m*-chi, and (c) Yamaguchi decomposed images of different scatterings (red: double-bounce scattering, green: volume scattering, and blue: surface scattering) obtained for the Barkot Forest area.

Upon comparison, it was found that the *m*-chi decomposition shows the higher correlation, i.e., 0.4823. Even though this correlation is not very high, it has been found to be sufficiently closer to the earlier studies [7], [13], where the correlation was ∼0.43–0.49.

The plots used in the present article are quite homogeneous giving high field biomass. Due to the dense forest, the volume scattering comes out to be high leading to the high total backscatter. This gives high values of the modeled AGB which is calculated using the semiempirical model, i.e., EWCM. Hence, there exists a positive and linear correlation between the modeled AGB and field biomass.

Earlier the study conducted by Chandola [9] on biomass estimation shows that on the comparison between modeled biomass against field biomass, $R^2$ value was 0.496 using IWCM and 0.4625 (for the present article) using EWCM. The number of plots used in this article [9] was 45, while in the present article plots were increased to 49. The variations in results are also due to the different models used for the AGB estimation.

The backscattering from the upper canopy is plotted against field-measured AGB (see Fig. 6) to quantify the effect only due to volume scattering while modeling the AGB. The low value of $R^2$ is observed. However, the modeled AGB shows a higher correlation of 0.48 (see Fig. 5) with the field AGB because the EWCM uses other backscattering parameters, such as surface and double bounce in addition to sigma0veg as input. This indicates the capability of the proposed model to capture the different backscattering parameters to effectively model the AGB.

At last performance, analysis is done by calculating root mean square error (RMSE) for the modeled AGB with respect to the biomass measured in the field. Both the models (*m*-delta and

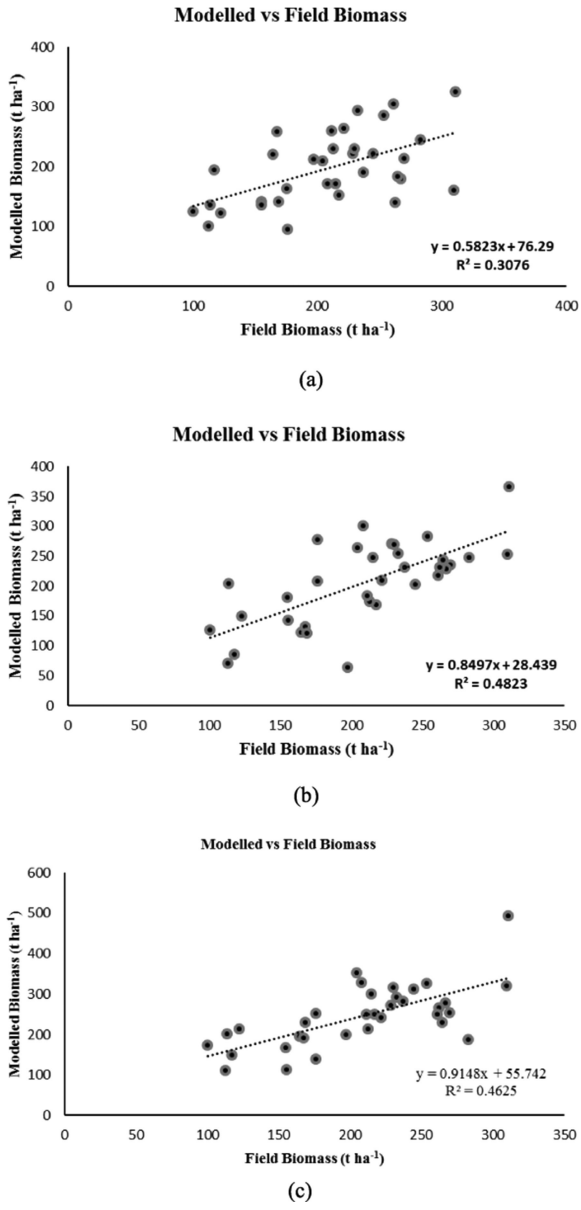


Fig. 5. Modeled AGB against field biomass using (a) *m*-delta decomposition, (b) *m*-chi decomposition, and (c) Yamaguchi decomposition.

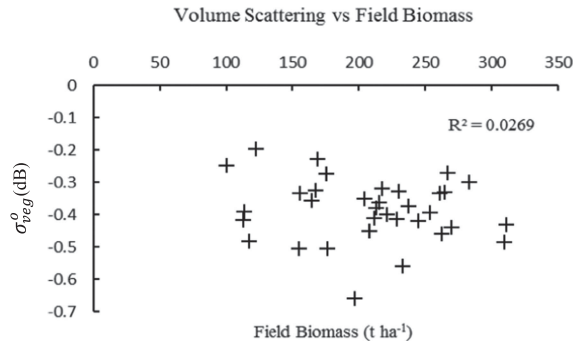


Fig. 6. Backscattering from the upper canopy layer ($\sigma^0_{\text{veg}}$) plotted against field biomass.

TABLE II
PERFORMANCE OF *M*-DELTA, *M*-CHI, AND YAMAGUCHI DECOMPOSITION TECHNIQUES IN BIOMASS ESTIMATION

| RMSE (t·ha$^{-1}$) | | | |
|---|---|---|---|
| | m-delta | m-chi | Yamaguchi |
| Overall | 55.302 | 50.145 | 67.266 |
| AGB<200 | 45.54 | 60.53 | 59.79 |
| AGB>200 | 60.55 | 42.45 | 79.19 |
| Overall % accuracy | | | |
| m-delta | m-chi | | Yamaguchi |
| 73.40 | 75.88 | | 67.65 |

*AGB is represented in t·ha$^{-1}$.

*m*-chi) underestimate the biomass. However, the decomposition model that performed better was the *m*-chi decomposition technique with RMSE of 50.145 (t·ha$^{-1}$). Similar studies for forest AGB estimation have reported similar RMSE (48 t·ha$^{-1}$) and higher RMSE (53–57 t·ha$^{-1}$) [17], [18]. The *m*-chi decomposition technique also performed significantly for the lunar surface in differentiating the even-bounce backscatter against the odd-bounce backscatter as concluded in the research article by Bhavya [19]. The performance analysis is summarized in Table II. The RMSE is calculated for the biomass range of 0–200 t·ha$^{-1}$, biomass >200 t·ha$^{-1}$, and overall. Due to the less dataset, only two categories have been assessed. Although both decomposition techniques perform differently for the biomass range between 0–200 and >200, no significant trend could be observed with the increase in biomass. Overall RMSE and % accuracy of m-chi outperforms m-delta. Table II indicates that more datasets are required to perform in-depth trend analysis for different biomass ranges. The variation in the results obtained from each decomposition may be due to the parameters (m, d, and $\chi$) considered for decomposition modeling.

The findings show that the *m*-chi performed better than the *m*-delta decomposition model for the AGB estimation. This is also supported by an earlier article for the lunar surface for the extraction of scattering elements using the *m*- delta and *m*-chi decomposition techniques, where it was demonstrated that the *m*-delta decomposition produced anomalous results in the retrieval of scattering elements [5], whereas the *m*-chi decomposition for the retrieval of scattering elements gave significant results [6].

## VI. CONCLUSION

In the present article, AGB has been estimated using the Hybrid Pol decomposition modeling and compared with the fully polarimetric decomposition technique. This article highlights the potential of Hybrid PolSAR for implying the decomposition modeling to estimate the AGB. WCM was used as the basis to retrieve the forest stand parameter, i.e., AGB by extending the model using the ground-to-stem interactions and applied in this article as EWCM. This model was trained using 15 plots

out of 49 plot data. The precise estimates of backscatter from vegetation, backscatter from the ground-to-stem interactions, and backscatter from the ground surface were obtained. The model well describes the relation of backscatter values with the field measured biomass.

AGB estimation using EWCM for the *m*-delta decomposition showed $R^2$ value of 0.3076. The estimated RMSE was found as 55.302 ($t{\cdot}ha^{-1}$). On the basis of the results obtained from this decomposition method, the accuracy was found to be 73.406%. The *m*-chi decomposition showed $R^2$ value as 0.4823 for the modeled biomass. The RMSE was calculated and found to be 50.145 ($t{\cdot}ha^{-1}$). The calculated accuracy for the *m*-chi decomposition was 75.88%. Since the RMSE value for the *m*-chi is lower and the accuracy is higher used in this article, hence *m*-chi outperformed *m*-delta decomposition. The Hybrid Pol decomposition technique outperformed the fully pol decomposition technique for the AGB estimation.

This article has also shown the capability of Hybrid Pol RISAT-1 *C*-band SAR dataset for the AGB estimation of Barkot Forest. Hybrid pol decomposition techniques studied in this article are m-chi and m-delta. Volume scattering was found to be dominant among the other scattering components in both the decompositions. Using EWCM-based semiempirical modeling for the AGB estimation, a higher correlation was obtained from the m-chi decomposition. Estimated biomass using m-chi decomposition is closer to the field measured biomass with an accuracy of 75.8%. Other modeling-based approaches at longer wavelengths could provide better understanding and improve the research work for increasing the consistency of decomposition modeling for the AGB estimation.

## REFERENCES


[1] J. Pajtík, B. Konôpka, and M. Lukac, "Biomass functions and expansion factors in young Norway spruce (Picea abies [L.] Karst) trees," *Forest Ecol. Manage.*, vol. 256, pp. 1096–1103, 2008.

[2] R. J. Williams, A. Zerihun, K. D. Montagu, M. Hoffman, L. B. Hutley, and X. Chen, "Allometry for estimating aboveground tree biomass in tropical and subtropical Eucalypt woodlands," *Aust. J. Botany*, vol. 53, no. 7, pp. 607–619, 2005.

[3] M. E. Nord, T. L. Ainsworth, J.-S. Lee, and N. J. S. Stacy, "Comparison of compact polarimetric synthetic aperture radar modes," *IEEE Trans. Geosci. Remote Sens.*, vol. 47, no. 1, pp. 174–188, Jan. 2009.

[4] A. Freeman and S. L. Durden, "A three-component scattering model for polarimetric SAR data," *IEEE Trans. Geosci. Remote Sens.*, vol. 36, no. 3, pp. 963–973, May 1998.

[5] R. K. Raney, J. T. S. Cahill, G. W. Patterson, and D. B. J. Bussey, "The m-chi decomposition of hybrid dual-polarimetric radar data," *J. Geophys. Res.*, vol. 117, no. E5, pp. 5093–5096, 2012.

[6] S. Saran, A. Das, S. Mohan, and M. Chakraborty, "Study of scattering characteristics of the lunar equitorial region using Chandrayaan-I Mini-SAR polarimetric data," *Planet. Space Sci.*, vol. 71, no. 1, pp. 18–30, 2012.

[7] Y. Yamaguchi, Y. Yajima, and H. Yamada, "A four-component decomposition of POLSAR images based on the coherency matrix," *IEEE Geosci. Remote Sens. Lett.*, vol. 3, no. 3, pp. 292–296, Jul. 2006.

[8] J. Lee and T. L. Ainsworth, "The effect of orientation angle compensation on coherency matrix and polarimetric target decompositions," *IEEE Trans. Geosci. Remote Sens.*, vol. 49, no. 1, pp. 53–64, Jan. 2011.

[9] S. Chandola, "Polarimetric SAR interferometry for forest aboveground biomass estimation," M.S. thesis, Fac. Geoinf. Sci. Earth Observ., Univ. Twente, Hengelosestraat, The Netherlands, 2014.

[10] R. K. Raney, "Hybrid-polarity SAR architecture," *IEEE Trans. Geosci. Remote Sens.*, vol. 45, no. 11, pp. 3397–3404, Nov. 2007.

[11] U. Khati, S. Kumar, and P. Thakur, "Effect of shift in polarization orientation angle on multi-wavelength fully polarimetric data," in *Proc. 9th Int. Conf. Microw., Antenna, Propag. Remote Sens.*, 2013, vol. 1, pp. 30–34.

[12] K. Dasari and A. Lokam, "Exploring the capability of compact polarimetry (Hybrid Pol) C band RISAT-1 data for land cover classification," *IEEE Access*, vol. 6, pp. 57981–57993, 2018.

[13] P. V. Jayasri *et al.*, "Implementation of RISAT-1 Hybrid polarimetric decomposition techniques and analysis using corner reflector data," *J. Indian Soc. Remote Sens.*, vol. 46, no. 6, pp. 1005–1012, 2018.

[14] S. Chirakkal, D. Haldar, and A. Misra, "Evaluation of hybrid polarimetric decomposition techniques for winter crop discrimination," *Prog. Electromagn. Res.*, vol. 55, pp. 73–84, 2017.

[15] P. S. Bharadwaj, S. Kumar, S. P. S. Kushwaha, and W. Bijker, "Polarimetric scattering model for estimation of above ground biomass of multilayer vegetation using ALOS-PALSAR quad-pol data," *Phys. Chem. Earth, A/B/C*, vol. 83–84, pp. 187–195, 2015.

[16] K. S. Tomar, S. Kumar, V. A. Tolpekin, and S. K. Joshi, "Semi-empirical modelling for forest above ground biomass estimation using hybrid and fully PolSAR data," *Proc. SPIE, Land Cryos. Remote Sens. III*, 2016, vol. 9877, 2016, Art. no. 987729.

[17] X. Huang, B. Ziniti, N. Torbick, and M. J. Ducey, "Assessment of forest above ground biomass estimation using multi-temporal C-band Sentinel-1 and polarimetric L-band PALSAR-2 data," *Remote Sens.*, vol. 10, no. 9, 2018, Art. no. 1424.

[18] N. Ghasemi, V. Tolpekin, and A. Stein, "Assessment of forest aboveground biomass estimation from PolInSAR in the presence of temporal decorrelation," *Remote Sens.*, vol. 10, no. 6, 2018, Art. no. 815.

[19] K. B. Bhavya, "Polarimetric modelling of the lunar surface for scattering information retrieval using Mini-SAR data of Chandrayaan-1," M.Sc. thesis, Fac. Geoinf. Sci. Earth Observ., Univ. Twente, Hengelosestraat, The Netherlands, 2013.


**Kiledar S. Tomar** received the M.Sc. degree in geoinformatics from ITC, University of Twente, Hengelosestraat, The Netherlands, and the Indian Institute of Remote Sensing, Indian Space Research Organisation, Dehradun, India.

He is currently working as a Project Scientist-B with the National Centre for Polar and Ocean Research, Vasco-da-Gama, India. His research interests include PolSAR, PolInSAR, and differential interferometric SAR (InSAR/DInSAR) with its application on aboveground biomass estimation, vegetation mapping, and glaciers velocity estimation.

**Shashi Kumar** received the M.Sc. degree in physics from Patna University, Patna, India, the M.Sc. degree in geoinformatics under the joint education program of the Indian Institute of Remote Sensing (IIRS), Indian Space Research Organisation, Dehradun, India, and ITC, University of Twente, Hengelosestraat, The Netherlands, and the Ph.D. degree from the Indian Institute of Technology, Roorkee, India.

He is currently a Scientist with IIRS. He is actively involved with the science team of NASA, ISRO, Synthetic Aperture Radar (SAR), and ISRO Chandrayaan-2 mission. He has worked as a member of SAR Task Group to develop SAR protocols for the forest carbon inventory of Indian forest under the USAID Forest-PLUS Technical Assistance Program. His research interests include SAR remote sensing with special emphasis on polarimetric SAR, polarimetric SAR interferometry, and SAR tomography for structural and biophysical characterization of manmade and natural features.

**Valentyn A. Tolpekin** received the M.Sc. degree in theoretical physics from Odessa State University, Odessa, Ukraine, and the Ph.D. degree in physics from ITC, University of Twente, Hengelosestraat, The Netherlands, in 2004.

He is currently an Assistant Professor with the Department of Earth Observation Science, ITC. His research interests include mathematical and statistical tools for satellite image analysis, including Markov random fields, super-resolution mapping, and support vector machines.